Interval analysis applied to dielectric spectroscopy:
a guaranteed parameter estimation

M. Aufray * **A. Brochier** ** **W. Possart** ***

*on leave to the CIRIMAT -Toulouse, France- IN University of Saarland,
Chair Adhesion and Interphases in Polymers, Gebäude C6-3, Postfach 15 11
50, 66041 Saarbrücken, Germany (e-mail: maelenn.aufray@ensiacet.fr)
** on leave to Geneva University -Switzerland- IN University of Saarland,
Chair Adhesion and Interphases in Polymers, Gebäude C6-3, Postfach 15 11
50, 66041 Saarbrücken, Germany (e-mail: adrien.brochier@unige.ch)
*** University of Saarland, Chair Adhesion and Interphases in Polymers,
Gebäude C6-3, Postfach 15 11 50, 66041 Saarbrücken, Germany (e-mail:
w.possart@mx.uni-saarland.de)*

Abstract Dielectric spectra of materials are often difficult to analyze since the common software algorithms and line shape functions do not always provide unambiguous data for the fitted parameters. In particular, this article deals with epoxy/ceramics nano-prepolymers studied by dielectric spectroscopy. In this situation, both system (the prepolymer with nanofillers) and method (the dielectric spectroscopy) are complex. Taking into account the experimental error of each data point in the measured dielectric spectrum, the sofware based on a global optimization algorithm which uses interval analysis, provides a confidence interval for every parameter of the dielectric function implemented in the software. Then, this software is able to deliver and guarantee the number of relaxation processes even if they are in part masked by other phenomena like conductivity or electrode polarization.

Keywords: Constraint satisfaction problems, Intervals, Nonlinear analysis, Set, Inversion, spectroscopy, Material

1. INTRODUCTION

Dielectric spectroscopy (DES) is widely applied to polymers, monomers and other insulating materials because it is an extremely effective method for characterizing the molecular dynamics over many orders of magnitude of time or frequency, respectively. It is based on the interaction of an external field with the electric dipole moment of the sample, often expressed by permittivity. In the measurement, the complex dielectric function

$$\varepsilon^*(\omega) = \varepsilon'(\omega) - i\varepsilon''(\omega) \qquad (1)$$

with the angular frequency ω, is measured at constant temperature. This function is called the dielectric spectrum. There are a number of different dielectric mechanisms, connected to the way a studied medium reacts to the applied field. Each dielectric mechanism is centred on its characteristic frequency, which is the reciprocal of the characteristic time of the process. In general, dielectric mechanisms can be divided into relaxation and resonance processes. Dielectric relaxations as a whole are the result of the movement of dipoles (dipole relaxation) and electric charges (ionic relaxation) due to an applied alternating field. Commonly, dielectric spectra are modelled by a sum of relaxation processes, but the choice of a reasonable physical model for the relaxator is critical. Most of the usual models, reviewed briefly in the introductory section, result from phenomenological considerations providing limited physical foundation. Moreover, the fitting algorithm turns out to be crucial in terms of reliability and unambiguity of the dielectric model function determined. Common softwares use least square ap-

proximation fitting algorithms which need initial values for the fit parameters. This could imply some predestination of the fit results. In previous work, a parameter estimation algorithm which is free of these limitations was developed by Brochier et al. [2010]. The new algorithm S.A.D.E. not only provides the chosen dielectric model function by a confidence interval for each model parameter like the frequency position and the intensity of all relaxations: it also indicates the number of relaxations that are necessary to model the measured spectrum.

1.1 The Dielectric Spectroscopy and its Models

The Debye [1929] relaxators describe the dielectric relaxation response of an ideal, non-interacting population of freely rotating dipoles to an alternating external electric field

$$\varepsilon^* = \varepsilon_\infty + \frac{\varepsilon_S - \varepsilon_\infty}{1 + i\omega\tau_0} = \varepsilon_\infty + \frac{\Delta\varepsilon}{1 + i\omega\tau_0} \qquad (2)$$

Where ε_S is the static permittivity ($\varepsilon_S = \lim_{\omega\to 0}\varepsilon'(\omega)$), ε_∞ is the optical dielectric constant ($\varepsilon_\infty = \lim_{\omega\to\infty}\varepsilon'(\omega)$) and τ_0 is the characteristic relaxation time of the medium. Let us note that the Debye model refers to a well-defined physical situation. All other relaxator models reported in the literature imply phenomenological modifications of the Debye relaxator without well-defined physical background. For example, the Havriliak-Negami (HN or Havriliak and Negami [1967]) equation

$$\varepsilon^* = \varepsilon_\infty + \frac{\varepsilon_S - \varepsilon_\infty}{(1 + (i\omega\tau_0)^\alpha)^\beta} \qquad (3)$$

is a mixture of the Cole and Cole [1941, 1942] and the Davidson and Cole [1950] equations, accounting for the asymmetry and broadness of the measured dielectric dispersion curve by the additional phenomenological parameters α and β. Developed to describe the dielectric relaxation of some polymers, the HN function is now one of the most popular models for dielectric relaxation although no exact physical meaning can still be given to the coefficients α and β.

Then, for dielectric spectra containing several relaxations, it is possible to sum a number of relaxation processes according to equation (2) or (3), i.e. irrespective of the model used : in our case, the measured ensemble of dielectric relaxations were depicted as a superposition of relaxation functions with equal shape, *e.g.* the Debye function. Here is the example, for r relaxations represented by the Debye model:

$$\varepsilon^* = \varepsilon_\infty + \sum_{j=1}^{r} \frac{\Delta\varepsilon_j}{1 + i\omega\tau_j}. \qquad (4)$$

At high temperatures and $\omega \to 0$, a contribution of a DC-conductivity (σ_{DC}) can be observed in the dielectric spectra of real polymer samples. It contributes only to the imaginary part of the measured complex dielectric permittivity, as long as the imaginary part of the generalized complex conductivity can be neglected in the low frequency region (i.e. $\sigma'' \ll \varepsilon'$). With this presumption, the following equation links the measured quantities $\tilde{\varepsilon}'$, $\tilde{\varepsilon}''$ to the true dielectric material quantities ε', ε'' and the DC electric conductivity (σ_{DC}):

$$\tilde{\varepsilon}'(\omega) = \varepsilon'(\omega) \text{ and } \tilde{\varepsilon}''(\omega) = \varepsilon''(\omega) + \frac{\sigma_{DC}}{\omega\varepsilon_0} \qquad (5)$$

At high frequencies, the contribution from the DC-conductivity becomes negligible and hence

$$\lim_{\omega \to \infty} \tilde{\varepsilon}''(\omega) = \varepsilon''(\omega) \qquad (6)$$

At low frequencies, the ε'' term is negligible compared to σ_{DC}, leading to the following equation (Mangion et al. [1992], Corezzi et al. [1997], Axelrod et al. [2004], Stickel et al. [1996]).

$$\lim_{\omega \to 0} \tilde{\varepsilon}''(\omega) = \frac{\sigma_{DC}}{\omega\varepsilon_0} \qquad (7)$$

However, some relaxations can take place even at these low frequencies. They are very difficult to fit using classical approaches (i.e. common algorithms) because they can be masked by the DC-conductivity.

As a consequence, the fitting process has to lead to a set of parameters which makes the model to fit both the real and the imaginary part, and has to detect hidden relaxations.

Electrode polarization is a parasitic effect in dielectric experiments which can mask the pure dielectric response of the sample material shown by Fuoss and Kirkwood [1941]. Moreover, as described by Maxwell [1954], Wagner [1914], Sillars [1937] (MWS polarization), phases in heterogeneous media are to be treated as macroscopic volume elements with different ε^* and conductivities σ^*. The experimental example presented in previous work (Brochier et al. [2010]) reveals that the MWS polarization causes a strong rise both in the real part (where electrode polarization is more visible) and in the imaginary part

of the permittivity (where the electrode polarization superimposes to the DC-conductivity) with decreasing frequency. In this work, the electrode polarization will be modeled by one strong Debye relaxator (recall that the MWS equation is very similar to the Debye equation). The only way to separate all the phenomena (electrode polarization, DC-conductivity, and maybe low-frequency dielectric material relaxations) is a simultaneous fit of the real and imaginary part of the permittivity using a formula taking all these phenomena into account.

1.2 Modeling problems: simultaneous fit and choice of the model

The main problem is that different physical processes can occur at the same frequency and temperature: the example of some small relaxations hidden by the DC-conductivity is very clear. Therefore, the only way to separate the phenomena is a simultaneous fit of the real and imaginary part of the permittivity. So the simple fit of the imaginary part of the permittivity (used by most of researchers, except Axelrod et al. [2004]) does not give a good solution as relaxations or other phenomena can be missed. The fit of the complex function of the permittivity will be done by our algorithm S.A.D.E. presented in the next paragraphs. Interval analysis has already been shown to be very efficient for solving hard modelization problems. In particular, interval methods have been successfully applied in Raïssi et al. [2004, 2005] to the modelization of an artificial set of data generated using the Havriliak-Negami model, as well as to the modelization of real conductivity and diffusivity measurements in Braems et al. [2005]. The relaxations and the electrode polarization are fitted by the Debye model (the only one model with a physical meaning), and the DC-conductivity by its specific function. Of course, we cannot determine *ex ante* the number of Debye relaxations needed to fit our curves, but the program S.A.D.E. will try to fit the curve using from 1 to r relaxations and one term due to DC-conductivity.

$$\varepsilon^* = \varepsilon_\infty + \sum_{j=1}^{r} \frac{\Delta\varepsilon_j}{1 + i\omega\tau_j} - i\frac{\sigma_{DC}}{\omega\varepsilon_0} \qquad (8)$$

The goal of the data fitting is to find the parameter values of the applied physical model that match the data most closely. The models to which the data are fitted depend on adjustable parameters. Therefore, the fitting process requires both the choice of a physical model and the choice of a suitable computing algorithm. Most of the scientific softwares fit experimental data by using some variants of the least squares approximation method but the success of the fit is not guaranteed. A different algorithm will be presented which makes the fit by the Debye model of experimental data with several relaxations possible in an efficient way, even if some of them are hidden.

2. INTERVAL ANALYSIS AND DATA FITTING

S.I.V.I.A. (Set Inversion Via Interval Analysis) is a set inversion algorithm introduced by Jaulin and Walter [1993a,b]. The algorithm is able to find a suitable approximation of the set of solutions of a constraints satisfaction problem, that is a set of the form

$$S = \{x \in \mathbb{R}^k \mid \forall i = 1\dots n, f_i(x) \in [y_i]\}$$

where each $f_i : \mathbb{R}^k \to \mathbb{R}$ is a given function and each $[y_i] = [y_i^-, y_i^+] \subset \mathbb{R}$ is a given interval. The approximation of S is given as a list of boxes $([b_i])_{i=1\dots N}$. A box is a Cartesian product of k

intervals (hence, in particular, it is a subset of $\mathbb{R}^k$), and the list returned by SIVIA satisfies

$$S \subset \bigcup_{i=1}^{N} [b_i]$$

It turns out that data fitting problems in a *bounded error context* can be interpreted as constraints satisfaction problems: let $(x_i, y_i)_{i=1...n}$ be a set of experimental data, and assume that the measurement accuracy is known. Hence, to each y_i is associated an interval $[y_i] = [y_i - e_i, y_i + e_i]$ where e_i is the measurement error. Let $f(x, p)$ be a physical model depending on a vector of parameters $p \in \mathbb{R}^k$. In this situation, it is natural to assume that a given vector of parameters p^* leads to a "good" fit if it is consistent with the measurement errors, that is if

$$\forall i \in \{1, ..., n\}, \ f(x_i, p^*) \in [y_i]$$

Such a vector of parameters is called feasible. Letting $f_i(p) = f(x_i, p)$, the set of feasible parameters is precisely

$$P = \{p \in \mathbb{R}^k \mid \forall i \in \{1, ..., n\}, \ f_i(p) \in [y_i]\}$$

Interval analysis makes possible the computation with intervals rather than with real numbers, and thus it leads to a very similar criterion for checking whether a box contains feasible parameters. Thus, by cutting the space in which feasible parameters are searched into finitely many small pieces in a suitable way, it is possible to compute a precise approximation of P. This is exactly what SIVIA is designed for.

First of all, elementary real operations are extended to intervals according to the following formula:

$$[x] \circ [y] = \{x \circ y \mid x \in [x], y \in [y]\} \text{ for } \circ \in \{+, -, *, /\} \quad (9)$$

Arithmetic operations with boxes are defined componentwise. The size of an interval $[x] = [x^-, x^+]$ is defined by:

$$Size([x]) = x^+ - x^- \quad (10)$$

The size of a box is the size of its greatest component. A bisection procedure will also be used, which cuts a box into two parts and returns the two parts. For a given box $[p] = ([p_1], [p_2], ..., [p_k])$, the procedure finds the index i of the greatest component, and returns 2 boxes:

$$([p_1], [p_2], ..., [p_i^-; p_i^- + (p_i^+ - p_i^-)/2], ..., [p_k]) \quad (11)$$

and

$$([p_1], [p_2], ..., [p_i^- + (p_i^+ - p_i^-)/2; p_i^+], ..., [p_k]) \quad (12)$$

Let us keep in mind that we do not always get an interval when we calculate the image of an interval by a real function. Hence, let

$$f : \mathbb{R} \longrightarrow \mathbb{R} \quad (13)$$

be a real function. Let $\mathbb{IR}$ be the set of intervals, a so-called "inclusion function" for f is an interval function

$$[f] : \mathbb{IR} \longrightarrow \mathbb{IR} \quad (14)$$

which verifies

$$\forall [x] \in \mathbb{IR}, \ f([x]) \subseteq [f]([x]) \quad (15)$$

In other word, the image of an interval (or a box) $[x]$ by an inclusion function for f is always still an interval (or a box) which contains the true image of $[x]$. In order to guarantee that $[f]$ is a suitable approximation of f, the following two conditions are also required:

$$\forall [x], [y] \in \mathbb{IR}, \ [x] \subseteq [y] \Rightarrow [f]([x]) \subseteq [f]([y]) \quad (16)$$

$$\forall ([x_n])_{n \in \mathbb{N}} \in \mathbb{IR}^{\mathbb{N}}, \ (Size([x_n]) \to 0)$$
$$\Rightarrow (Size([f]([x_n])) \to 0) \quad (17)$$

Of course, there are infinitely many inclusion functions for a given real function. One of them is minimal but could be difficult to find. Then, the so-called natural inclusion function will be used. The natural inclusion function is simply obtained by replacing each operator in the associated real function by its interval equivalent, and each usual function $(\sin, \cos, \exp, \sqrt{\ })$ by a suitable interval counterpart.

Now let $[f](x, [p])$ be an inclusion function associated with the physical model $f(x, p)$ and call a box $[p^*]$:

- feasible if $\forall i = 1 ... n, \ [f](x_i, [p^*]) \subset [y_i]$
- unfeasible if $\exists i \in \{1, ..., n\}, \ [f](x_i, [p^*]) \cap [y_i] = \emptyset$
- indeterminate otherwise

Let $[P_0]$ be a box big enough to contains P and $\eta > 0$ be a small number, the precise description of SIVIA is given by figure 1.

```
List L
Stack S
Push(S,[P0])
While Not( isEmpty(S) )
    [pc] ← Pop(S)
    If [pc] is feasible
        Push(L,[pc])
    End If
    If [pc] is indeterminate
        If Size([pc]) ≤ η
            Push(L,[pc])
        Else
            {[p1],[p2]}=Bisection([pc])
            Push(S,[p1])
            Push(S,[p2])
        End If
    End If
End While
Return L
```

Figure 1. S.I.V.I.A. (Set Inversion Via Interval Analysis)

In the case of a data fitting problem, however, a precise approximation of P by a list of boxes is not needed. One would rather like to have a confidence interval for each parameter, which amounts to find an approximation of the *bounding box* of P, that is of the smallest box containing P. To this end, instead of pushing every feasible box into a list, the algorithm should take the convex union of this box and the current result. The convex union of two boxes is the bounding box of their ordinary union. Hence, the returned value is not a list anymore but a single box, which decrease the occupied memory space. Another side effect is that, as the convex union is bigger (in the sense of the inclusion) than the usual one, it may happen that a box is already contained in the current result without having been processed. Testing this before processing a box saves a lot of computation time.

However, the Debye model (8) has some symmetries which makes the bounding box of P not relevant. Indeed, this function is invariant under any permutation of the couples (ε_i, τ_i), meaning that P is made of several connected components, each of which are identical up to some permutation of the coordinates. Hence, it is necessary to select one of the connected component. It can be done by assuming that

$$\forall i \in \{1, ..., r-1\}, \ \tau_i < \tau_{i+1}$$

As the algorithm deals with intervals, this constraint cannot be applied directly. However, it is obvious that this relation implies that the upper bound of $[\tau_i]$ cannot be greater than the upper bound of $[\tau_{i+1}]$, and conversely the lower bound of $[\tau_{i+1}]$ cannot be smaller than the lower bound of $[\tau_i]$. So the algorithm will remove some (and potentially all) values from $[\tau_i]$ by using:

$$\text{For } i = 1 \text{ To } r-1, \quad [\tau_i] \leftarrow [\tau_i^-; \min(\tau_i^+, \tau_{i+1}^+)] \quad (18)$$

and

$$\text{For } i = 1 \text{ To } r-1, \quad [\tau_{i+1}] \leftarrow [\max(\tau_i^-, \tau_{i+1}^-); \tau_{i+1}^+] \quad (19)$$

Again, there is a positive consequence of that. The size of $[\tau_i]$ could decrease by this process, or $[\tau_i]$ could become empty. Obviously, there are much more parameters which do not satisfy this constraint than parameters which do, so a lot of boxes will be simply removed during this process (namely, when $\tau_{i+1}^+ < \tau_i^-$, or when $\tau_i^- > \tau_{i+1}^+$ for some i) even if they are mathematically feasible, decreasing considerably the computing time.

Due to the "branch and bound" nature of SIVIA, the computing time grows exponentially with the number of parameters. In order to make it applicable in the most complicated situations, a two-pass approach was used. First, the original SIVIA algorithm, together with the procedure which select a single connected component, is applied by freezing all the parameters but the τ_i's. It means that size tests and bisections are performed only with respect to the τ_i's. Even with a small value of η, it returns very quickly (usually in a few seconds) a list of boxes leading to a coarse approximation of P. This first pass remove large parts of the initial search space. Then, taking the above list as an input, a second pass is performed using our modified algorithm involving the convex union. Real cases experiments shows that this simple trick decreases the computing time a lot.

By using these modifications (which, except the last one, were described by Brochier et al. [2010]), it was possible to give a new algorithm, S.A.D.E. (as S.I.V.I.A. Applied to DiElectric spectroscopy) having many nice properties compared to traditional methods. If there are no parameters satisfying the constraints, then it will return an empty set, leading to a very strong criterion to determine the number of relaxations, which is generally not known in advance. All the returned parameters belong to the initial search space. So there is no risk to find nonsense parameters, such as negative values. It is possible to add some arbitrary constraints that the parameters have to satisfy. It is also possible to use in only one step, several systems of constraints coming from different sources (for example to fit simultaneously the real and imaginary part of a set of data) or to use several sets of data coming from repeated measurements (data accumulation) in order to increase the quality of the result. It leads to an interval for each parameter, which is guaranteed to contain the true parameter value, and which size is directly linked to the measurement accuracy.

3. DES APPLIED ON NANOFILLED EPOXY-AMINE SYSTEMS AND RESULTS USING S.A.D.E.

As the DES is widely applied in the characterization of polymers (Kremer and Schönhals [2003], Gregoriou [2004], Fawcett [1996], Runt and Fitzgerald [1997]), the nanocomposites (very fashioned polymers since 10 years) can be studied by DES (Valentini et al. [2004], Yudin et al. [2005], Zhang

et al. [2006]). In this situation, both system (polymer with nanofillers) and method (the dielectric spectroscopy) are complex: that is probably why such study are not so often related. Calorimetry, mechanic testing, and rheology were more used than the DES. The DES results are comparable with rheology results: the influences of the surface state of the fillers, their percentage… were correlated with the transition of the networks.
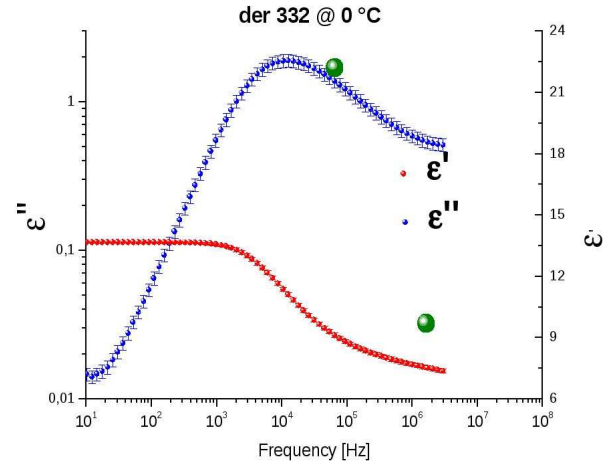

Figure 2. Dielectric Spectroscopy real and imaginary permittivity of the DGEBA DER 332 prepolymer at 0°C and the corresponding two Debye relaxations as calculated by S.A.D.E.
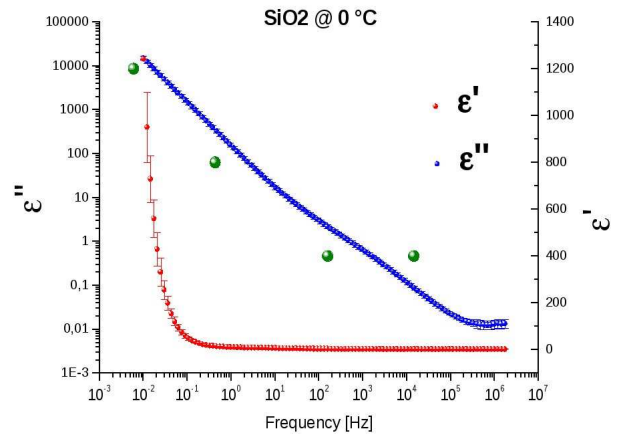

Figure 3. Dielectric Spectroscopy real and imaginary permittivity of the SiO_2 nano-fillers and the corresponding four Debye relaxations as calculated by S.A.D.E.

Part of nanocomposites were made of epoxy-amine polymer filled with nanofillers (Valentini et al. [2004], Zhang et al. [2006]). Most used nanofillers are clays, carbon (nanotubes), or carbon coated nanofillers, but only few articles deals with epoxy-amine/ceramics nanocomposites. That is why such a study would be very interesting, particularly if it was coupled with a modeling of our results (as the modeling add a difficulty, no study was investigated to model the nanocomposite materials).

The pure diglycidylether of bisphenol A (DGEBA) DER 332 from DOW Chemical was studied by dielectric broadband measurements in a frequency range of 0.1 Hz to 10^6 Hz using a Novocontrol High Resolution Dielectric Alpha Analyser with automatic temperature control by a Quatro cryosystem. For the

examples presented here, 200 data points were measured in the frequency range at 0°C.

The viscous DGEBA was placed between stainless steel electrodes, with a PTFE spacer in order to have a well-defined geometry.

A Dual Opteron machine containing two 2.4 GHz/64 Bits CPUs and at least 4 GB of RAM was used. The operating system was Suse Linux 10.0. A parallelized version of the algorithm was implemented (in the C++ programming language) in order to take advantage of the two CPUs.

The experiment was run on a DER 332 well known system, filled by SiO_2 (GLYMO, from Hartwig et al. [2005]).

The figures 2 and 3 show ε' and ε'' measured at 0°C, for pure der 332 and pure SiO_2 nanofillers, whereas the figure 4 shows ε' and ε'' measured at 0°C for the epoxy der 332 DGEBA filled with nano-SiO_2. By eyes, as a first approach, only one relaxation can be detected on the pure and nano-filled der 332 epoxy (Figures 2 and 4). Only conductivity and electrode polarization are detectable for nanofillers, without epoxy (Figure 3). On the figures 2, 3 and 4 the relaxations found by SADE (green points) are represented too. Let us note that these relaxations were not visible on the dielectric spectrum and not possible to fit by classical ways (particularly for the SiO_2, figure 3). The ordinate were changed in order to be able to represent epsilon', epsilon" and the SADE results on the same graph. In addition, ε_∞ and σ_{DC} are not represented here, as ε_∞ has no real meaning, and the σ_{DC} variation is more interesting versus temperature. Let us note that S.A.D.E. tries first to fit these data points by only one Debye relaxator. As the fit failed, it tries with two (Fig. 2) to five (Fig. 4) relaxations: using five Debye relaxators lead to the determination of eleven parameter intervals! If we try to fit the data points with more than 5 relaxations, the additional relaxations will be masked by the measurement errors. Then, the numbers of relaxations provided by S.A.D.E. is considered as optimum. It is worth noting that these parameters were not found by classical least square approximation fitting routines.

Of course, the results presented on the figures 2, 3 and 4 are not perfect: for the sake of simplicity, the Debye relaxations found by S.A.D.E. were represented by the green point whereas they are vectors of intervals. Anyway, the comparison of the
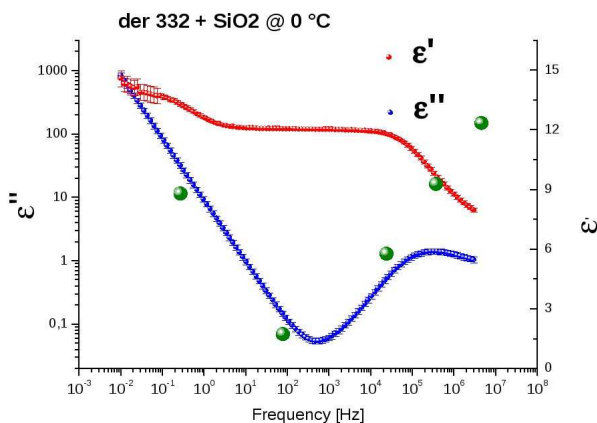
relaxation for the three systems is very interesting. The relaxations appearing between the DGEBA without and with SiO_2 are exactly the SiO_2 relaxations (whereas it was commonly thought that a ceramic cannot have any relaxation. These likely results lead us to develop again our algorithm S.A.D.E. in order to perfectly identify relaxations and conductivity.

4. CONCLUSION

Dielectric spectroscopy is an extremely versatile method for characterizing the molecular dynamics over a large range of time scales. Unfortunately, the extraction of model parameters by data fitting is still a crucial problem which is now solved by our program S.A.D.E.

S.A.D.E. is based on the algorithm S.I.V.I.A. which was proposed and implemented by Jaulin and Walter [1993a,b] in order to solve constraint satisfaction problems. The problem of dielectric data analysis is reduced to a problem of choosing the appropriate physical model. In this article, Debye relaxations were used and validated to fit the relaxations of a DGEBA prepolymer and the polarization of the spectrometer electrodes. The conductivity was evaluated too.

S.A.D.E. is now able to split a complex DES spectra into a guaranteed number of Debye relaxations.

5. SOFTWARE AVAILABILITY

S.A.D.E. is freely available at:
http://www.unige.ch/~brochier/sade.php
S.A.D.E. is protected by copyright (c) 2006 Brochier, and is distributed under the terms of the GNU general public license.

REFERENCES

N Axelrod, E Axelrod, A Gutina, A Puzenko, P Ben Ishai, and Y Feldman. Dielectric spectroscopy data treatment; i. frequency domain. *Meas. Sci. Technol.*, 15:1–10, 2004.

I. Braems, N. Ramdani, A. Boudenne, M. Kieffer, L. Jaulin, L. Ibos, E. Walter, and Y. Candau. New set-membership techniques for parameter estimation in presence of model uncertainty. In *Proceedings 5th Int. Conf. Inverse Problems In Engineering: Theory & Practice*, volume 1, page B09. Cambridge, Leeds University Press, Leeds, 2005.

A. Brochier, M. Aufray, and W. Possart. *Materials with Complex Behaviour*, chapter Dielectric Spectra Analysis: Reliable Parameter Estimation Using Interval Analysis, pages 99–123. WILEY, 2010.

Kenneth S. Cole and Robert H. Cole. Dispersion and absorption in dielectrics. i. alternating current characteristics. *J. Chem. Phys.*, 9:341–351, 1941.

Kenneth S. Cole and Robert H. Cole. Dispersion and absorption in dielectrics. ii. direct current characterisctics. *J. Chem. Phys.*, 10:98–105, 1942.

S Corezzi, S Capaccioli, G Gallone, A Livi, and P.A. Rolla. Dielectric behaviour versus temperature of a monoepoxide. *J. Phys.: Condens. Matter*, 9:6199–6216, 1997. URL http://www.fisica.unipg.it/~corezzi/.

D.W. Davidson and Robert H. Cole. Dielectric relaxation in glycerine. *J. Chem. Phys.*, 18:1417–1417, 1950.

P. Debye. *Polar molecules*. Chemical Catalog, Reprinted by Dover Publications, New York, 1929.

Allan H. Fawcett. *Polymer Spectroscopy*. Wiley-VCH, 1996.

Figure 4. Dielectric Spectroscopy real and imaginary permittivity of the DGEBA DER 332 prepolymer at 0°C filled with SiO_2 nano-fillers and the corresponding five Debye relaxations as calculated by S.A.D.E.

Raymond M. Fuoss and John G. Kirkwood. Electrical properties of solids. viii. dipole moments in polyvinyl chloride-diphenyl systems. *J. Am. Chem. Soc.*, 63(2):385–394, 1941.

V. G. Gregoriou. *Polymer Spectroscopy*. Number 1–272. Wiley-VCH, 2004.

A. Hartwig, M. Sebald, and M. Kleemeier. Cross-linking of cationically polymerised epoxides by nanoparticules. *Polymer*, 46:2029–2039, 2005.

S. Havriliak and S. Negami. A complex plane representation of dielectric and mechanical relaxation processes in some polymers. *Polymer*, 8:161–210, 1967. URL `http://www.sciencedirect.com/science/article/B6TXW-48FBVVM-4T/2/ffb6daa2b39f773a1666f9d2cb8d4ed8`.

Luc Jaulin and Eric Walter. Set inversion via interval analysis for nonlinear bounded-error estimation. *Automatica*, 29(4):1053–1064, July 1993a. URL `http://www.sciencedirect.com/science/article/B6V21-47WVRTR-5T/2/35ab6e2405d16f0886be1fcfc21d687c`.

Luc Jaulin and Eric Walter. Guaranteed nonlinear parameter estimation from bounded-error data via interval analysis. *Math. Comput. Simul.*, 35(2):123–137, April 1993b. URL `http://www.sciencedirect.com/science/article/B6V0T-45DHW9D-2/2/f8024c6b00508f6f3ce7087b39f78f59`.

F. Kremer and A. Schönhals. *Broadband Dielectric Spectroscopy*. Springer, Berlin, 2003.

M.B.M Mangion, M. Wang, and G.P. Johari. Relaxations in thermosets. xii. dielectric effects during curing of nonstoichiometric dgeba-based thermosets. *J. Polym. Sci., Part B: Polym. Phys.*, 30(5):433–443, 1992. URL `http://www3.interscience.wiley.com/cgi-bin/fulltext/104051384/PDFSTART`.

J.C. Maxwell. *A Treatise on Electricity and Magnetism*. Number 1. Dover publications, New York, 1954.

T. Raïssi, L. Ibos, N. Ramdani, and Y. Candau. Guaranteed method for the estimation of dielectric relaxation models parameters. In *8th IEEE International Conference On Solid Dielectrics ICSD*. Toulouse, 2004.

T. Raïssi, N. Ramdani, L. Ibos, and Candau Y. A reliable method for the estimation of dielectric relaxation models parameters. In *Proceedings Of The 5th Int. Conf. Inverse Problems In Engineering: Theory & Practice*, volume III, page R01. Cambridge, Leeds University Press, Leeds, 2005.

J. P. Runt and J. J. Fitzgerald. *Dielectric Spectroscopy of Polymeric Materials: Fundamentals and applications*. American Chemical Society: Washington DC, 1997.

R.W. Sillars. The properties of a dielectric containing semi-conducting particles of various shapes. *Proc. Instn. Elect. Engrs.*, 80:378–394, 1937.

F. Stickel, E.W. Fischer, and R. Richert. Dynamics of glass-forming liquids. ii. detailed comparison of dielectric relaxation, dc-conductivity, and viscosity data. *J. Chem. Phys.*, 104(5):2043–2055, 1996.

L. Valentini, D. Puglia, E. Frulloni, I. Armentano, J.M. Kenny, and S. Santucci. Dielectric behavior of epoxy matrix/single-walled carbon nanotube composites. *Composites Science and Technology*, 64(1):23–33, January 2004. URL `http://www.sciencedirect.com/science/article/B6TWT-48YVWDC-D/2/6b849474c2e0ab36e7d28581cad9f0e8`.

Karl Willy Wagner. Erklärung der dielektrischen nachwirkungsvorgänge auf grund maxwellscher vorstellungen. *Archiv für Elektrotechnik*, 2(9):371–387, 1914. URL `http://www.springerlink.com/content/xr0617448810/?p=a72f93d829804c93afa018301302e470&pi=624`.

V.E. Yudin, G.M. Divoux, J. U. Otaigbe, and V. M. Svetlichnyi. Synthesis and rheological properties of oligoimide/montmorillonite nanocomposites. *Polymer*, 46(24):10866–10872, 2005.

Bangwen Zhang, Changsheng Xie, Junhui Hu, Huihu Wang, and YangHai Gui. Novel 1-3 metal nanoparticle/polymer composites induced by hybrid external fields. *Composites Science and Technology*, 66(11-12):1558–1563, 2006. URL `http://www.sciencedirect.com/science/article/B6TWT-4J3WGJD-1/2/e1f5302b886ba699f19bc75fd9296f3b`.